Investigation of Mechanism and Critical Parameters for Removal of Arsenic from Water using Zr-TiO$_2$ Composite

I. Anđelković, N. R. R. Amaizah, S. B. Marković, D. Stanković, M. Marković, D. Kuzmanović & G. Roglić

Accepted author version posted online: 02 Nov 2016.

Submit your article to this journal ⎘

Article views: 1

View related articles ⎘

View Crossmark data ⎘

Investigation of Mechanism and Critical Parameters for Removal of Arsenic from Water using Zr-TiO₂ Composite

I. Anđelković [a, *], N. R. R. Amaizah [b], S. B. Marković [c], D. Stanković [a], M. Marković [d], D. Kuzmanović [e], G. Roglić [e]

ᵃ Innovation center of the Faculty of Chemistry, University of Belgrade, Studentski Trg 12-16, Belgrade, Serbia

ᵇ Department of Chemistry, Faculty of Art & Sciences, Al-Mergeb University, P.O. Box 40397/40414, Al-Khums, Libya

ᶜ Institute of Technical Sciences of the Serbian Academy of Sciences and Arts, Knez Mihailova 35/IV, Belgrade, Serbia

ᵉInstitute of Chemistry, Technology and Metallurgy, Center of Chemistry, University of Belgrade, Njegoseva 12, Belgrade, Serbia

ᵉ Faculty of Chemistry, University of Belgrade, Studentski Trg 12-16, Belgrade, Serbia

*Corresponding author: ivanhem@chem.bg.ac.rs

Phone: +61 420 532 086

Abstract

Using microwave-hydrothermal method for synthesis of composite, high surface density of hydroxyl groups, as an active adsorption sites for arsenic, was obtained. Adsorption mechanisms of As(III) and As(V) onto zirconium doped titanium-dioxide (Zr-TiO₂) was investigated and proposed using macroscopic and microscopic methods. Obtained results are suggesting inner-sphere and outer-sphere adsorption mechanisms for As(III) and As(V), respectively. This allowed us identification of parameters that are critical for the successful removal of arsenic from water, essential information for further optimization of the removal process. Composite was further applied for the removal of As(III) and As(V) from water in a dynamic flow through reactor. Column study proved that removal of both arsenic species below value recommended by WHO

1

can be achieved. Elution of As(III) and As(V) from the composite can be done by using small amount of 0.01 M NaOH solution resulting in preconcentration of arsenic species and possible multiple usage of composite.

1. Introduction

Adsorption is considered as one of the best available techniques for removal of arsenic from aqueous systems. Simplicity of technological process, the possibility of applying to individual households and low cost of the treatment led to increased efforts of the scientific community in order to find the best possible sorbent which can be used in adsorption. [1,2] Until now, as adsorbents, many naturally available and waste materials were tested for removal of pollutants from the environment. As a criteria in the selection of natural or waste material which will be examined for the removal of arsenic were abundance, local availability and low price. Among tested materials were red mud [3], sea nodule [4], biochars derived from rise husk, organic solid waste and sewage sludge [5]. The use of natural or waste materials is usually limited by the low capacity of adsorption, narrow effective pH range of application and negative effect of coexisting ions on removal process. However, in recent years there is an evident increase in the number of papers dealing with the synthesis of materials, which will have as many desirable characteristics that are necessary for material application in the control of environmental pollution. [2,6] The research was going in the direction of synthetic materials that can be synthesized from inexpensive and readily available raw materials with method that is fast, simple and which can be easily scaled up for synthesis in an industrial scale. The most important part of the adsorption process is adsorbent itself, usually used in the column process. As a starting point of the research, a certain properties should be achieved in order for the material to be used in the column processes, such as: the appropriate size of pores (porosity), large number functional groups with high affinity to the desired pollutants, the availability of these active centers to polluted medium. Having this in mind, researchers devoted considerable attention to the composite materials obtained by combining metal oxides. By combining two or more metal oxides some scientists observed that new composite not only inherits the desired properties from parent compounds but shows obviously synergistic effect. [7] Thus the substantial number of binary oxides was synthesized that have been tested for the removal of pollutants from the water. In the synthesis of composites, elements that are usually combined are the ones that have an affinity for the pollutants with the elements that possess the mechanical and chemical resistance, such as Fe-Mn [8], Ce-Zr [9], Fe-Zr [10] and Fe-Cu [11] binary oxides for the removal of phosphates, Sn-Mn [12] and Zr-Mn [13] for removal of mercury, Fe-Mn [14] for removal of cobalt, Al-Si [15] and Fe-Mn [16] for removal of selenium.

Increased concentrations of As in drinking water, since its discovery more than twenty years ago, is one of the biggest environmental problem that humanity is facing. [17] A variety of materials were tested for arsenic removal, both natural and synthesized, whereby the efficiency of the sorbent followed the trend of the discovery of new materials synthesized by various techniques. [6, 18-22] Peng et al. [23] recently synthetized, using controlled double-jet precipitation technique, magnetic $Fe_3O_4@Cu(OH)_2$ composite, for the removal of As(V) from solution. Nanostructured iron(III)-copper(II) binary oxide [24] and iron-zirconium binary oxide [25], synthetized using simple precipitation method, showed promising results in batch removal studies which recommend these materials for column studies..

Andjelkovic et al. [19] have demonstrated that using microwave-hydrothermal procedure for synthesis of bimetallic oxide, $Zr-TiO_2$, a potentially good material for removal of arsenic from water was obtained. Titanium dioxide based materials are relatively well established materials for arsenic removal [17] while zirconium, as a doping element, was chosen based on its unique selectivity towards polyoxy anions and the fact that this element in its hydrated form can generate species which have abundant hydroxyl ions. [26] The microwave-hydrothermal procedure is simple, environmental friendly method for large scale production of materials which are more uniform in size and composition. Comparing with conventional hydrothermal method, in microwave-hydrothermal synthesis microwave energy diffuses in the sample resulting in higher reaction rate, more efficient usage of energy and higher yield of product. [27] The aim of this work is to study the mechanism of sorption of arsenic onto bimetallic oxide in order to determine the factors that are responsible for arsenic removal. Knowledge of the mechanisms of sorption allows us to synthesize materials with specific properties and optimize the removal procedure. Efficiency of arsenic removal with column process, as the next step towards commercial application of this material, was examined.

2. Material and methods

All chemical and reagents used in this study were of analytical grade. Stock solutions (1000 mg/L) of As(III) and As(V) were prepared by dissolving appropriate amount of $NaAsO_2$ (Fisher Scientific, USA) and $Na_2HAsO_4 \cdot 7H_2O$ (Fluka, Spain) in deionized water, respectively.

2.1. Adsorbent preparation

The $Zr-TiO_2$ composite was prepared according to the microwave-hydrothermal method described in detail in publication [19]. Briefly, $TiCl_4$ was added to ice cooled deionized water ($TiCl_4:H_2O$(v/v) ratio 1:10) where homogeneous and transparent solution was obtained. Then, $ZrCl_4$ was added to solution to give 10% of dopant and solution was subjected to precipitation by the slow addition of 30 % NH_4OH under constant stirring at room temperature. The hydrolysis was controlled with the addition of NH_4OH until reaction mixture attained pH between 7 and 8. The suspension was transferred into a Teflon microwave closed vessel (digestion system ETHOS 1 Milestone, equipped with a High Pressure Rotor SK-, Italy), sealed and heated by microwave

3

irradiation reaching a maximum temperature of 150° C in 10 minutes, the kept at this temperature for 15 minutes more for hydrothermal treatment. The resulting product was separated by centrifugation and washed repeatedly with deionized water until precipitate became free of chloride ion. Finally, it was dried at 80° C for 5 h. Synthetized adsorbent, TiO_2 doped with zirconium, was labeled as $Zr-TiO_2$.

2.2. Characterization of the sorbent

Scanning electron microscopy (SEM) was used to examine the morphology of synthetized material. The SEM analysis was conducted on a JEOL microscope model JSM-6610LV.

X-ray powder diffraction (XRPD) was used for identification of crystalline phases. The XRPD patterns were collected with Philips diffractometer PW1710 employing CuKα radiation. Step scanning was performed with 2θ ranging from 20 to 100°, step size of 0.10° and the fixed counting time of 5 s per step.

Adsorption–desorption isotherms were obtained by nitrogen adsorption at -196° C using a Sorptomatic 1990 Thermo Finnigan device. Prior to adsorption, the sample was degassed for 1 h at room temperature under vacuum and additionally 16 h at 110° C at the same residual pressure. The specific surface area of sample (S_{BET}) was calculated by applying the Brunauer–Emmet–Teller equation, from the linear part of the adsorption isotherm. [28] The total pore volume (V_{tot}) was obtained from the N_2 adsorption, expressed in liquid form, by applying Gurevitsch's rule. [29] Micropore volume (V_{mic}) was estimated according to the Dubinin–Radushkevich method. [30] Mesopore volume (V_{mes}) was estimated according to the Barrett, Joyner and Halenda method from the desorption branch of the isotherm (Barrett et al. 1951). [31]

2.3. Determination of surface hydroxyl density

A procedure developed by Muller et al. [32] was adapted for determination of surface OH density using thermogravimetic analysis. The thermal behavior was determined by simultaneous TG–DTA (Setsys, SETARAM Instrumentation, Caluire, France) in the temperature range between 25 and 500 °C under the air flow of 20 ml min^{-1}, in an Al_2O_3 pan. The heating profile was set as follows: the material was stabilized at 25 °C for 5 min then heated to 120 °C with the heating rate of 10 °C min^{-1} and with dwell time of 30 min. The materials were then heated to 500 °C with the heating rate of 20 °C min^{-1}. The surface hydroxyl group density (D_{OH}, OH nm^{-2}) was calculated based on weight loss (g) between 120 °C and 500 °C using Eq. 1.

$$D_{OH} = \alpha \left(\frac{\omega t_{T_1} - \omega t_{T_2}}{\omega t_{T_1}} \right) \frac{2N_A}{S_{BET} \times M_{wH_2O}} \quad \text{(Eq. 1)}$$

where α = 0.625 (calibration factor), T_1=120 °C and T_2=500 °C, N_A is Avogadro's number and S_{BET}(nm^2 g^{-1}) is the BET surface area (S_{BET}=114 m^2/g, see [19]) and M_{wH_2O} is the molecular weight of water.

2.4. Determination of PZC

The point of zero charge (PZC) was determined in accordance with procedure described by Babic et al. [33] Accordingly, the samples of Zr-TiO$_2$ (0.20 g) in 0.01 M NaCl solution with pH adjusted at different pH values were shaken in plastic vials for 24 h. Initial pH values were obtained by adding an amount of NaOH or HCl solution (0.1M). After equilibration, pH values of filtered suspensions were measured.

2.5. FTIR study

The adsorption samples for FTIR spectra were prepared by treating of material with 10 mg/L of As(III) at pH 9 and 10 mg/L of As(V) at pH 3 for 24 h. Experiments were done at specified pH values because former study [see 19] indicated that highest adsorption of As(III) and As(V) were achieved at pH 9 and 3, respectively. The FTIR spectra were measured in the form of KBr pellets on a Nicolet 6700 FTIR (Thermo Scientific, USA)

2.6. Column adsorption experiments

Dynamic flow adsorption tests of As(V) and As(III) using were carried out individually using transparent glass column of 1.0 cm inner diameter and 12 cm length with glass filter at the bottom. The weighted amount (200 mg) of Zr-TiO$_2$ was transferred carefully, with small amount of deionized water into the column, minimizing void space and cracks in bed. Test solution, containing 200 µg/L of As(III) or As(V) at pH 5.6, was passed through column in a down flow manner using ISM796 (ISMATEC, Switzerland) pump. Beforehand, column was conditioned by passing of deionized water at the same pH for 12 h. Collected samples of arsenic were analyzed with ICP-MS (iCAP Qc Thermo Scientific, Germany). Flow rate used for As(V) and As(III) were 1.0 and 0.7 ml/min, respectively.

3. Results and Discussion

The morphology of Zr-TiO$_2$, presented in Fig.1a, shows sponge-like surface of material. Presence of large number of small particles on the surface of the composite, which results in rough, porous surface, should be beneficial to the sorption process. EDX results (Fig.1b) confirms successful incorporation of Zr at the surface of the composite.

Figure 1

The XRD spectra of Zr-TiO$_2$ (Fig. 2) shows that the most intensive diffraction peaks can be ascribed to the anatase crystal structure (JCPDS card 78-2486). Absence of diffraction peaks that could be described to the doped Zr are probably result of the incorporation of Zr ions in the crystal structure of TiO$_2$ or formation of small clusters which have size too low in order to be identified with the diffractometer.

Figure 2.

Physical properties of TiO$_2$, synthetized by the same procedure as Zr-TiO$_2$ but without addition of Zr, and Zr-TiO$_2$ are presented in Tab.1. Large specific surface area provides a larger number of active sites available for adsorption while size of micro and meso-pores determines the kinetic of adsorption. As we can see from Tab. 1, all physical properties which are preferable for the fast and high removal of pollutants from water, increased in Zr-TiO$_2$ composite in comparison to TiO$_2$, indicating positive effect of doping of Zr to TiO$_2$.

Table. 1.

Material	TiO$_2$	Zr-TiO$_2$
Pore volume (Gurvich) at /p$_0$, cm^{3}g^{-1}	**0.226**	**0.390**
Specific surface area, m^{2}g^{-1}	**65**	**114**
Mesopores (B.J.H.) desorption, Stand. Lecloux, Cumulative pore volume, cm^{3}g^{-1}	**0.302**	**0.360**
Micropore volume (Dubinin and Raduskevich), cm^{3}g^{-1}	**0.018**	**0.034**

3.1.Density of OH groups

The surface of metal oxides suspended in aqueous solution is commonly described as a hydroxylated surfaces formed by the dissociation of water molecules on metal atoms of the surfaces. [34] These hydroxyl (OH) groups are regarded as active adsorption sites for arsenic adsorption and their density and availability have substantial effect on the efficiency of the removal process. [35] For used composite material, there are two different OH groups which can act as an active sites for As(III) and As(V) adsorption, Zr−OH and Ti−OH groups. Possible reason for achieved efficient removal of both arsenic species could be high density of OH groups of Zr doped TiO$_2$ obtained by microwave-hydrothermal process. In order confirm this, surface OH density was determined by using thermogravimetric analysis developed by Mueller et al. [32] Based on TGA data, presented in Fig. 3, calculated surface density of OH groups for Zr−TiO$_2$ was 11.64 nm^{-2}. This value was 50 % higher than the highest value obtained for TiO$_2$/ZrO$_2$ composite synthetized using sol-gel template technique. [36] Obtained density of surface OH groups goes in favor to the statement that microwave-hydrothermal method is an efficient technique of synthesis of material with dense number of OH groups which are responsible for adsorption of arsenic.

Figure 3

3.2.Change of PZC

The point of zero charge is defined as the condition at which the surface charge density, independent of ionic strength and determined in the presence of inert electrolyte, equals zero. Determined PZC of the material was 6.8 ± 0.2 and at this value equal amount of positive and negative surface charge are present. After treatment of the material for 24 h with 10 ppm of As

(III) at pH 9 and 10 ppm of As(V) at pH 3, obtained PZC for Zr-TiO$_2$ treated with As(III) and As(V) were 6.3±0.2 and 6.7±0.2, respectively (Fig. 2). As PZC of metal oxides is determined by protonation and deprotonation of surface hydroxyl groups, formation of outer-sphere surface complexes cannot shift the PZC because there are no specific chemical reactions between the adsorbed species and surface that could change surface charge. [37] However, the formation of inner-sphere surface complexes, through covalent or ionic bonding of chemical species directly onto the surface of adsorbent, could shift PZC to the lower pH values. [37] Therefore, results of PZC determination after adsorption of As(III) onto Zr-TiO$_2$ suggest that As(III) formed negatively charged, inner-sphere surface complex. No significant change in PZC of Zr-TiO$_2$ after As(V) adsorption suggest formation of outer-sphere surface complex by attaching As(V) for the adsorbent surface indirectly through the one or more water molecules or formation of inner-sphere surface complex that does not change the surface charge. [38, 39]

Figure 4

3.3. FTIR results

FTIR analysis was done in order to identify stretching and bending motions of functional groups at the surface of the material after adsorption of As(III) and As(V). Myneni et al. [40] evaluated the vibrational spectroscopy of As(V) sorbed on mineral surfaces using theoretical and experimental studies, with emphasis on the protonation, hydratation and metal complexation influence on the As-O symmetric stretching vibrations. In Fig. 3 are represented FTIR spectra of Zr-TiO$_2$ after adsorption of As(V) and As(III). Obtained peaks for As(V) adsorption, 743 and 732 cm^{-1} could be ascribed to symmetric and asymmetric As-OH stretching vibration of H$_2$AsO$_4^-$, arsenate specie present in the pH 3. [40] The presence of As-OH band below 760 cm^{-1} and absence of As-OM, where M represents either Ti or Zr, around 810 cm^{-1} in the spectra indicates that adsorbed As(V) is protonated.

Figure 5

Possible mechanism of As(V) adsorption onto Zr-TiO$_2$ at pH 3 is represented in Fig. 4. FTIR spectra of Zr-TiO$_2$ composite after As(V) adsorption, combined with no significant shift of PZC of material after adsorption of As(V), suggests indirect attachment of arsenate ions to the surface of the adsorbent through water molecule, i.e. formation of outer-sphere complex of arsenate to Zr-TiO$_2$ surface.

Figure 6

In contrast to As(V), identification of adsorption bands of As(III) after adsorption is more difficult because the possibility of oxidation of arsenite to arsenate. Although oxidation mechanism of As(III) by TiO$_2$ has been investigated in last 10 years there is still no clear conclusion about the mechanism. Wei et al. [41] proposed surface superoxide (or hydroperoxy radical) should have the main role in the oxidation process while Ferguson et al. [42] with selective use of hydroxyl radical

quenchers and superoxide dismutase demonstrated that superoxide radical plays a major role in the oxidation of As(III) to As(V). From the Fig. 3 small peak at 780 can be observed, which can be attributed to stretching vibration of an uncomplexed As-O bands in $(TiO)_2AsO^-$ complex. The presence of uncomplexed As-O bond suggest that the As(III) surface complex was not protonated [43] This complex could contribute to the decrease of PZC observed after adsorption of As(III). Combining macroscopic experiment with spectroscopic method gave us a base for inner-sphere bidentate, binuclear adsorption mechanism of As(III) on $Zr-TiO_2$ composite represented in Fig. 5. This As(III) surface mechanism is in agreement with previous studies of As(III) adsorption on titanium, iron and aluminum oxides. [43-45]

Figure 7

3.4. Column experiments

The ability of $Zr-TiO_2$ composite material in dynamic flow conditions was studied by passing arsenic solutions through a column. Initial concentration of arsenic and flow rate for column experiments was chosen based on the pervious batch experiments and conditions necessary to meet the practical needs in treatment of drinking water. Results represented in Fig. 6 show breakthrough profiles, of As(III) and As(V). From this figure it can be seen that the breakthrough point (10 µg/L of arsenic in effluent) for As(III) and As(V) were 45 and 60 bed volumes (BV), respectively. After treatment of 320 BV of water containing 200 µg/L As(V) 50 % until saturation of sorbent was achieved while after passing 400 BV of water containing the same initial concentration of As(III) this percent was 77. Reason for higher efficiency of $Zr-TiO_2$ towards As(III) could be initial pH of treated solutions which is more favorable for removal of As(III) than As(V).

Figure 8

Ability of sorbent to regenerate is highly desirable quality from economic and ecological point of view. In order to test regeneration of used composite 0.01 M NaOH solution was used as eluent of adsorbed arsenic. From Fig. 7 we can see more than 6 and 3.5 fold enrichment in concentration of As(V) and As(III), respectively, using only 3 ml of 0.01 M NaOH solution. This results are in accordance with proposed mechanisms for As(III) and As(V) in which later, physisorbed is more easily desorbed from composite than former inner-sphere, chemisorbed complex.

Figure 9

Experimental results presented here are in good agreement with previous studies of the mechanism of arsenic adsorption and arsenic removal with column process showing importance of surface OH groups in arsenic adsorption. [46, 35] Column experiments have shown possible application of Zr-TiO_2 for removal of As(III) and As(V) from water. Further studies of column process using

experimental design, in order to optimize the most important experimental parameters, should be performed in future.

4. Conclusion

In pursuit of material that will effectively remove arsenic from water, using microwave-hydrothermal method for synthesis of $Zr-TiO_2$ composite we have shown that density of surface OH groups, as active adsorption centers for removal of arsenic, was substantially higher than using sol-gel technique. Shifts in point of zero charge with adoption of As(III) and As(V) together with FTIR spectra's of material after adsorption of As(III) and As(V) suggests outer-sphere adsorption mechanism for As(V) and inner-sphere mechanism for As(III). Due to slower formation of the inner-sphere, bidentate, binuclear complex during As(III) adsorption, contact time of solution with the material seems like the most important parameter that influences the removal process. In the case of As(V), because of the electrostatic attraction of As(V) and sorbent as a dominant mechanism of removal, initial pH of the solution, which influences surface charge of the adsorbent, has the greatest effect on the removal process. Preliminary tests showed that removal of both arsenic species below value recommended by WHO was achieved in column study. Preconcentration of As(III) and As(V) was done with small amount of 0.01M NaOH solution desorbing arsenic from column and creating possibility for composite to be used multiple time.

References

[1] Kowalski PK. Chemistry of Advanced Environmental Purification Processes of Water. Elsevier: Oxford, UK, 2014 Chapter 8, Advanced Arsenic Removal Technologies Review; p. 285-337.

[2] Ungureanu G, Santos S, Boaventura R, Botelho C. Arsenic and antimony in water and wastewater: Overview of removal techniques with special reference to latest advances in adsorption. J. Enviro. Manage. 2015; 151: 326-342.

[3] Soner Altundogan H, Altundogan S, Tumen F, Bildik M. Arsenic removal from aqueous solutions by adsorption on red mud. Waste Manage. 2000; 20: 761-767.

[4] Maity S, Charkravarty S, Bhattacharjee, Roy BC. A study on arenic adsorption on polymetallic sea nodule in aqueous medium. Water Res. 2005; 39: 2579-2590.

[5] Agrafioti E, Kalderis D, Diamadopoulos E. Arsenic and chromium removal from water using biochars derived from rice husk, organic solid wastes and sewage sludge. J. Environ. Manage. 2014; 133: 309-314.

[6] Mohan D and Pittman Jr. CU. Arsenic removal from water/wastewater using adsorbents - A critical review. J. Hazard. Mater. 2007; 142: 1-53.

[7] Zhang G, Ren Z, Zhang X, Chen J. Nanostructured iron(III)-copper(II) binary oxide: A novel adsorbent for enhanced arsenic removal from aqueous solutions. Water Res. 2013; 47: 4022-4031.

[8] Lu J, Liu H, Zhao X, Jefferson W, Cheng F, Qu J. Phosphate removal from water using freshly formed Fe-Mn binary oxide: Adsorption behaviors and mechanisms. Colloids Surf., A. 2014; 455: 11-18.

[9] Su Y, Yang W, Sun W, Li Q, Shang JK. Synthesis of mesoporous cerium-zirconium binary oxide nanoadsorbents by a solvothermal process and their effective adsorption of phosphate from water. Chem. Eng. J. 2015; 268: 270-279.

[10] Long F, Gong JL, Zeng GM, Chen L, Wang XY, Deng JH, Niu QY, Zhang HY, Zhang XR. Removal of phosphate from aqueous solution by magnetic Fe-Zr binary oxide. Chem. Eng. J. 2011; 171: 448-456.

[11] Li G, Gao S, Zhang G, Zhang X. Enhanced adsorption of phosphate from aqueous solution by nanostructured iron(III)-copper(II) binary oxides. Chem. Eng. J. 2014; 235: 124-131.

[12] Xie J, Xu H, Qu Z, Huang W, Chen W, Ma Y, Zhao S, Liu P, Yan N. Sn-Mn binary metal oxides as non-carbon sorbent for mercury removal in a wide-temperature window. J. Colloid Interface Sci. 2014; 428: 121-127.

[13] Xie J, Qu Z, Yan N, Yang S, Chen W, Hu L, Huang W, Liu P. Novel regenerable sorbent based on Zr-Mn binary metal oxides for flue gas mercury retention and recovery. J. Hazard. Mater. 2013; 261: 206-213.

[14] Jiang L, Xiao S, Chen J. Removal behavior and mechanism of Co(II) on the surface of Fe-Mn binary oxide adsorbent. Colloids Surf., A. 2015; 479: 1-10.

[15] Chan YT, Kuan WH, Chen TY, Wang MK. Adsorption mechanism of selenate and selenite on the binary oxide systems. Water Res. 2009; 43: 4421-4420.

[16] Xie W, Liang Q, Qian T, Zhao D. Immobilization of selenite in soil and groundwater using stabilized Fe-Mn binary oxide nanoparticles. Water Res. 2015; 70: 485-494.

[17] Abejon R and Garea A. A bibliometric analysis of research on arsenic in drinking water during the 1992-2012 period: An outlook to treatment alternatives for arsenic removal. Journal of Water Process Engineering, 2015; 6: 105-119.

[18] Minovic T, Gulicovski J, Stoiljkovic M, Jokic B, Zivkovic Lj, Matovic B, Babic B. Surface characterization of mesoporous carbon cryogel and its application in arsenic (III) adsorption from aqueous solutions. Microporous Mesoporous Mater. 2015; 201: 271-276.

[19] Andjelkovic I, Jovic B, Jovic M, Markovic M, Stankovic D, Manojlovic D, Roglic G. Microwave-hydrothermal method for synthesis of composite materials for removal of arsenic from water. Environ. Sci. Pollut. Res. 2016; 23: 469-476.

[20] Andjelkovic I, Manojlovic D, Skrivanj S, Pavlovic M, Amaizah N, Roglic G. As(III) and As(V) sorption on MnO_2 synthesized by mechano-chemical reaction from aqueous phase. Int. J. Environ. Res. 2013; 7: 395-402.

[21] Attinti R, Sarkar R, Barrett KR, Data R. Adsorption of arsenic(V) from aqueous solutions by goethite/silica nanocomposite. Int. J. Environ. Sci. Tech. 2015; 12: 3905-3914.

[22] Beduk F. Superparamagnetic nanomaterial Fe_3O_4-TiO_2 for the removal of As(V) and As(III) from aqueous solutions. Environ. Tecnol. 2016; 37: 1790-1801.

11

[23] Peng B, Song T, Wang T, Chai L, Yang W, Li X, Li C, Wang H. Facile synthesis of $Fe_3O_4@Cu(OH)_2$ composites and their arsenic adsorption application. Chem. Eng. J. 2016; 299: 15-22.

[24] Zhang G, Ren Z, Zhang X, Chen J. Nanostructured iron(III)-copper(II)binary oxide: A novel adsorbent for enchanced arsenic removal from aqueous solutions. Water Res. 2013; 47: 4022-4031.

[25] Ren Z, Zhang G, Paul Chen J. Adsorptive removal of arsenic from water by an iron-zirconium binary adsorbent. J. Colloid Interf. Sci. 2011; 358: 230-237.

[26] Biwas BK, Inoue J, Inoue K, Ghimire KN, Harada H, Ohto K, Kawakita H. Adsorptive removal of As(V) and As(II) from water by a Zr(IV)-loaded orange waste gel. J. Hazard Mater. 2008; 154: 1066-1074.

[27] Yasemin C, Kamuran G, Seval A. Effect of deposition parameters on the structural properties of ZnO nanopowders prepared by microwave-assisted hydrothermal synthesis. Spectrochim. Acta A. 2015; 138: 617-622.

[28] Rouquerol F, Rouquerol J, Sing K. Adsorption by powders and porous solids, principles, methodology and applications. Academic Press, London, UK, 1999.

[29] Gregg SJ, Sing KSW. Adsorption, surface area and porosity. Academic Press, London, UK, 1982.

[30] Dubinin MM. Progress in surface and membrane science. Academic Press, New York, USA, 1975.

[31] Barrett EP, Joyner LG, Halenda PP. The determination of pore volume and area distributions in porous substances. I. Computations from nitrogen isotherms. J. Am. Chem. Soc. 1951; 73: 373-380.

[32] Muller R, Kammler HK, Wegner K, Pratsinis SE. OH surface density of SiO_2 and TiO_2 by thermogravimetric analysis. Langmuir. 2003; 19: 160-165.

[33] Babic M, Milonjic K, Polovina J, Kaludjerovic V. Point of zero charge and intrinsic equilibrium constants of activated carbon cloth. Carbon. 1999; 37: 477-481.

[34] Lomenech C, Simoni E, Drot D, Ehrhardt JJ, Mielczarski J. Sorption of uranium (VI) species on zircon: structural investigation of the solid/solution interface. J. Colloid Interf. Sci. 2003; 261: 221-232.

[35] Yu Y, Yu L, Chen JP. Introduction of an Yttrium-Manganese Binary Composite That Has Extremely High Adsorption Capacity for Arsenate Uptake in Different Water Conditions. Ind. Eng. Chem. Res. 2015; 54: 3000-3008.

[36] Kimling MC, Scales N, Hanley TL, Caruso RA. Uranyl-Sorption Properties of Amorphous and Crystalline TiO_2/ZrO_2 Millimeter-Sized Hierarchially Porous Beads. Environ. Sci. Technol. 2012; 46: 7913-7920.

[37] Stumm, W. Chemistry of the solid-water interface. Wiley-Interscience: New York; 1999.

[38] Krauskopf KB and Bird DK. Introduction to Geochemistry; 3rd edn. McGraw-Hill: Boston (MA); 1995.

[39] Goldberg S and Johnston CT. Mechanism of Arsenic Adsorption on Amorphous Oxides Evaluated Using Macroscopic Measurements, Vibrational Spectroscopy and Surface Complexation Modeling. J. Colloid Interf. Sci. 2001; 234: 204-216.

[40] Myneni SCB, Traina SJ, Waychunas GA, Logan TJ. Experimental and theoretical vibrational spectroscopic evaluation of arsenate coordination in aqueous solutions, solids, and at mineral-water interfaces. Geochim. Cosmochim. Acta. 1998; 62: 3285-3300.

[41] Wei Z, Zhang S, Pan Z, Liu Y. Theoretical studies of arsenite adsorption and its oxidation mechanism on a perfect TiO_2 anatase (1 0 1) surface. Appl. Surf. Sci. 2011; 258: 1192-1198.

[42] Ferguson MA, Hoffmann MR, Hering JG. TiO_2-Photocatalyzed As(III) Oxidation in Aqueous Suspensions: Reaction Kinetics and Effect of Adsorption. Environ. Sci. Technol. 2005; 39: 1880-1886.

[43] Pena M, Meng X, Korfiatis GP, Jing C. Adsorption Mechanism of Arsenic on Nanocrystalline Titanium Dioxide. Environ. Sci. Technol. 2006; 40: 1257-1262.

[44] Manning BA, Fendorf SE, Goldberg S. Surface structures and stability of arsenic(III) on goethite: Spectroscopic evidence for inner-sphere complexes. Environ. Sci. Technol. 1998; 32: 2383-2388.

[45] Arai Y, Elzinga EJ, Sparks DL. X-ray adsorption spectroscopic investigation of arsenite and arsenate adsorption at the aluminum oxide-water interface. J. Colloid. Interf. Sci. 2001; 235: 80-88.

[46] Hu X, Ding Z, Zimmerman AR, Wang S, Gao B. Batch and column sorption of arsenic onto iron-impregnated biochar synthesized through hydrolysis. Water Res. 2015; 68: 206-216.

Table captions:

Table 1. Physical properties of TiO_2 and $Zr-TiO_2$ materials

Figure captions:

Figure 1(a). SEM image of $Zr-TiO_2$

Figure 1(b). EDX surface analysis of $Zr-TiO_2$

Figure 2. XRD pattern of $Zr-TiO_2$ composite

Figure 3. TGA curve of the $Zr-TiO_2$ composite

Figure 4. Comparison of pH_{PZC} of pristine $Zr-TiO_2$ and $Zr-TiO_2$ after adsorption of As(III) and As(V)
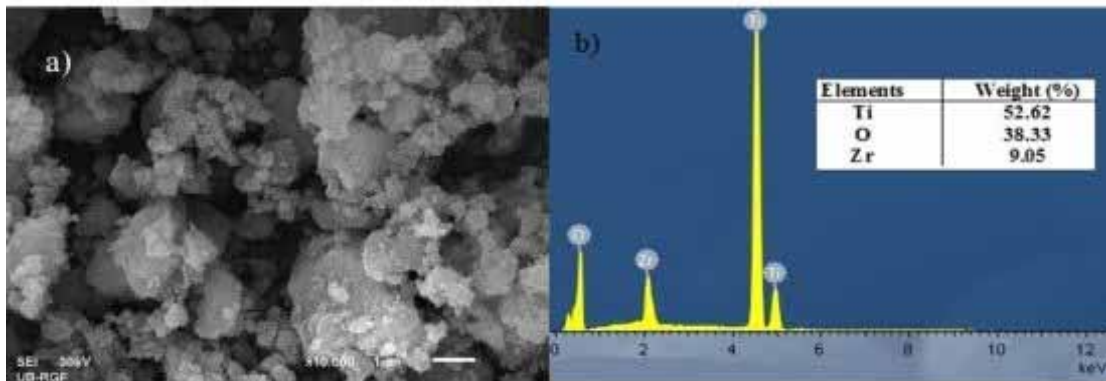
Figure 5. FTIR spectra of As(III) and As(V) adsorbed on $Zr-TiO_2$ at pH 9 and 3, respectively

Figure 6. Proposed mechanism for As(V) adsorption on $Zr-TiO_2$ composite at pH 3. The M represents either Zr or Ti

Figure 7. Proposed mechanism of As(III) on $Zr-TiO_2$ composite at pH 9. The M represents either Ti or Zr

Figure 8. Column adsorption tests for As(III) and As(V) onto $Zr-TiO_2$ composite at pH 5.6, where Ct and Co represent the concentration of arsenic in the effluent at time, t, and the initial concentration, respectively

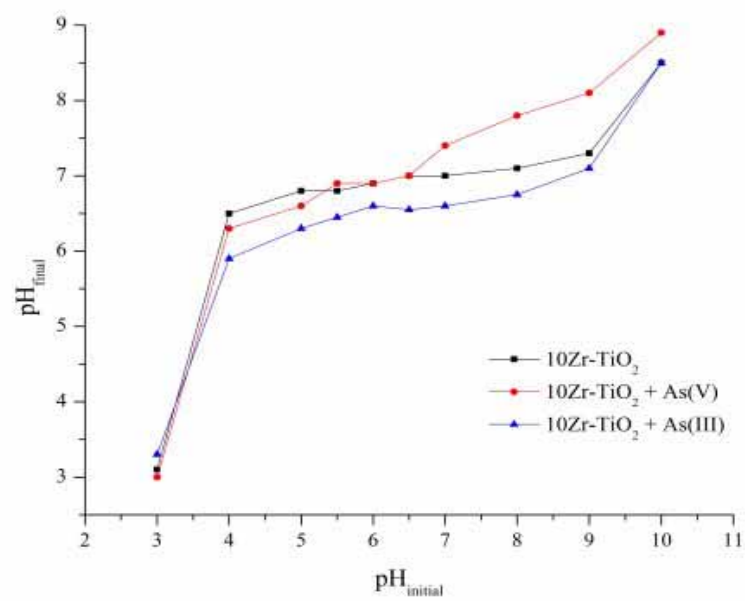Figure 9. Elution profiles for As(III) and As(V)

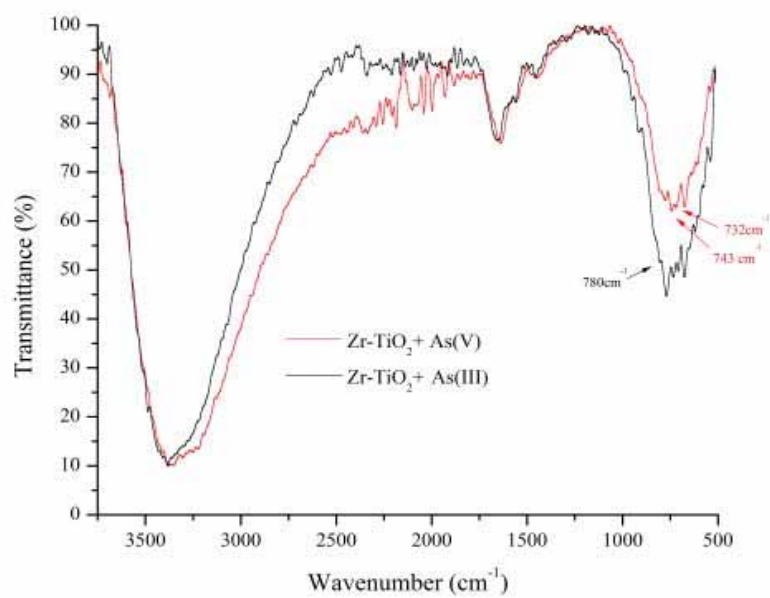| Elements	Weight (%)
Ti	52.62
O	38.33
Z r	9.05

= M (Ti or Zr)

= As

= O

= H